

Unsupervised Learning of Depth and Ego-Motion from Panoramic Video

Alisha Sharma
University of Maryland, University College
Adelphi, MD
lee@leesharma.com

Jonathan Ventura
California Polytechnic State University
San Luis Obispo, CA
jventu09@calpoly.edu

Abstract—We introduce a convolutional neural network model for unsupervised learning of depth and ego-motion from cylindrical panoramic video. Panoramic depth estimation is an important technology for applications such as autonomous robotic navigation, virtual reality, and 3D modeling. In contrast to previous approaches for applying convolutional neural networks to panoramic imagery, we use the cylindrical panoramic projection which allows for the use of the traditional CNN layers such as convolutional filters and max pooling without modification. Our evaluation on synthetic and real data shows that unsupervised learning of depth and ego-motion on panoramic images increases depth prediction accuracy in comparison to training on perspective images which have a narrower field-of-view.

I. INTRODUCTION

Understanding the structure of a 3D scene is an important problem in many fields, from autonomous vehicle navigation to 3D filming. Unfortunately, predicting 3D structure from a single image is extremely challenging. The number of confounding factors (e.g. varied texture, lighting, occlusions, and object movement) make it an ill-posed problem: a single image could represent many possible 3D scenes.

Early attempts at estimating scene structure from motion (also known as SfM) focused on directly analyzing factors such as the geometry and flow of the image [2], [18], [21]. However, these models were often fragile in the face of occlusions, object motion, and other inconsistent, but real-world, conditions. In the past several years, many exciting advances have been made in estimating scene structure and ego-motion—motion of the observer—using deep neural networks.

Early research relied on labelled data for training [7], [15]. Unfortunately, labeled 3D footage is expensive to create, limiting the quantity and diversity of available training data. This limitation has triggered a promising new area of research: unsupervised SfM models, which figure out scene attributes such as depth and ego-motion without requiring labeled data. In the past few years, several unsupervised models have been proposed with comparable performance to the supervised state-of-the-art [11], [30], [24], [16], [25], lowering the cost and expanding the diversity of potential training datasets.

While much progress has been made for “standard” pinhole perspective images, researchers have only recently started to apply these deep networks to panoramic input. There are many compelling applications for computer vision with non-pinhole projection images, such as robotic vision with omni-

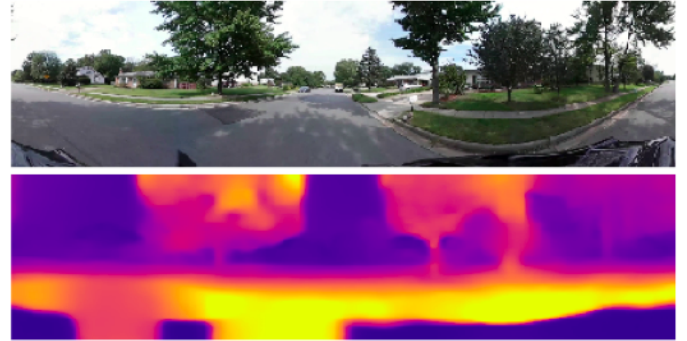


Fig. 1: An example of predicting depth (bottom) from a single panoramic input (top) using our proposed method. The depth is color-coded, so that brighter pixels are closer.

directional cameras. Spherical panoramas are interesting, but spheres cannot be perfectly mapped to a plane: any spherical projection model introduces distortions, requiring expensive modifications to the model layers [3], [8].

In contrast, cylindrical panoramas can be represented perfectly on a plane. They offer many of the same benefits as spherical panoramas, and standard convolutional layers can still be used (see Figure 2). Despite the advantages of cylindrical projection, to our knowledge, deep networks for depth prediction have not yet been applied to cylindrical panoramic imagery. Furthermore, all existing panoramic SfM CNN model require labeled data; no purely unsupervised panoramic SfM model has been proposed before.

In this paper, we address these gaps by proposing an unsupervised convolutional model that estimates depth and ego-motion from cylindrical panoramas.

This work has three major contributions:

- 1) We present CylindricalSfMLearner, an unsupervised model for estimating structure from motion given cylindrical panoramic input,
- 2) We demonstrate that training on panoramic input improves depth accuracy in comparison to training on perspective images, and
- 3) We provide a new dataset of panoramic street-level videos suitable for unsupervised learning of depth and ego-motion.

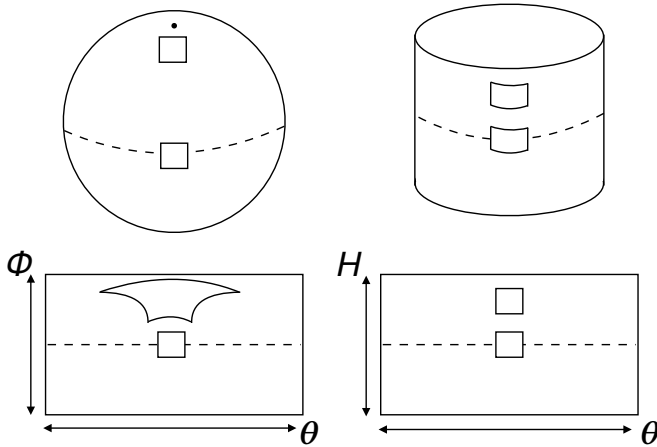


Fig. 2: Comparison of convolutional filtering on equirectangular panoramas (left) and cylindrical panoramas (right). A square area on the surface of the sphere (top left) maps to differently sized areas on the 2D image when using equirectangular projection (bottom left) [3]. In contrast, a square filter on cylindrical projection image (bottom right) always projects to the same area on the cylinder (top right). This property of cylindrical panoramas allows us to apply convolutional neural network layers to a cylindrical panorama without needing to model position-dependent effects on the receptive field, as in previous works [4], [23], [29].

II. RELATED WORK AND BACKGROUND

A. Supervised Monocular Depth Prediction

Early research focused on detecting structure from *stereo*—or multi-source—imagery. Stereo SfM is much more constrained than detecting structure from *monocular*—single-source—input, but the stereo input requirement limits the model’s flexibility. Eigen [7] proposed a different approach using deep neural networks. They presented a supervised model for estimating depth maps from monocular input images. Their model was composed of two stacks – one for coarse estimation and one for fine estimation – and joined the two predictions.

B. Supervised to Unsupervised Models

While supervised models for single-image depth prediction demonstrate excellent performance, collecting labeled footage is very expensive, increasing training cost and limiting the size and diversity of datasets. This limitation triggered a number of researchers to turn towards unsupervised models. Godard, taking inspiration from previous stereo techniques, proposed a model that was trained on unlabeled stereo footage. Their trained model outperformed the previous supervised state-of-the-art on urban scenes and reasonably well on unrelated datasets [11].

Zhou removed the constraint of stereo training footage. They proposed an unsupervised model composed of jointly-trained depth and pose CNNs using a loss function tied to novel view synthesis. They found that their unsupervised

model performed comparably to supervised models on the known datasets and reasonably well when tested against a completely unknown data set. Unfortunately, while the model could be trained on monocular footage, it assumes a given camera calibration, which prevents random footage from the web from being used as training data [30].

In a concurrent study, Vijayanarasimhan addressed this shortcoming by explicitly modeling scene geometry. Inspired by geometrically-constrained Simultaneous Localization and Mapping (SLAM) models and Godard’s work on left-right consistency, they proposed a model capable of detecting both ego-motion and object motion—as well as depth and object segmentation—from uncalibrated monocular images [24]. Building upon Zhou’s and Vijayanarasimhan’s models, Mahjourian proposed a completely unsupervised model with explicit geometric scene modeling [16]. Their model introduced a new 3D loss function and added a new principled mask for handling unexplainable input.

C. Beyond Pinhole Projection

All of the models previously discussed take pinhole images as input. However, pinhole images have a serious disadvantage: objects can move out of the field of view. Many applications, such as robotic navigation or virtual reality, benefit from the 360° field of view. Previous research tackled this omnidirectional SfM problem using direct methods with some success [12], but comparatively little research has been done with 360° imagery and CNNs.

Spherical input is particularly challenging for CNNs because spheres cannot be perfectly represented by a rectangular grid. In equirectangular projection, a common spherical projection method, this results in significant distortion in the polar regions of the image that propagate error through the convolutional layers. The traditional solution to this has been to use additional parameters and data augmentation to correct the distortions [14], but recently, researchers have presented a number of CNNs designed for direct spherical input. Several of these approaches aim for full rotational invariance by using signal processing techniques to model spherical convolutional layers [3], [8], [26]. While this approach is effective, it is also expensive; these models are severely limited in their input data size, making them impractical for most problems.

As full rotational invariance is often not required, several researchers have suggested a lighter-weight alternative: replacing normal convolutional filters with distortion-aware filters [4], [23], [29]. In this approach, the standard rectangular CNN filter is replaced by a filter that samples points based on the image distortion, correcting the polar distortion effects. These models can be trained with one projection model and tested with another, allowing them to utilize the large body of pinhole datasets. There were several other approaches aside from full rotational invariance and distortion-aware filters, including graph CNNs [13], style transfer [6], and increased filter sizes in the polar regions [22].

Cylindrical projection is another way of achieving 360° views around a given axis. Unlike spherical panoramas, cylin-

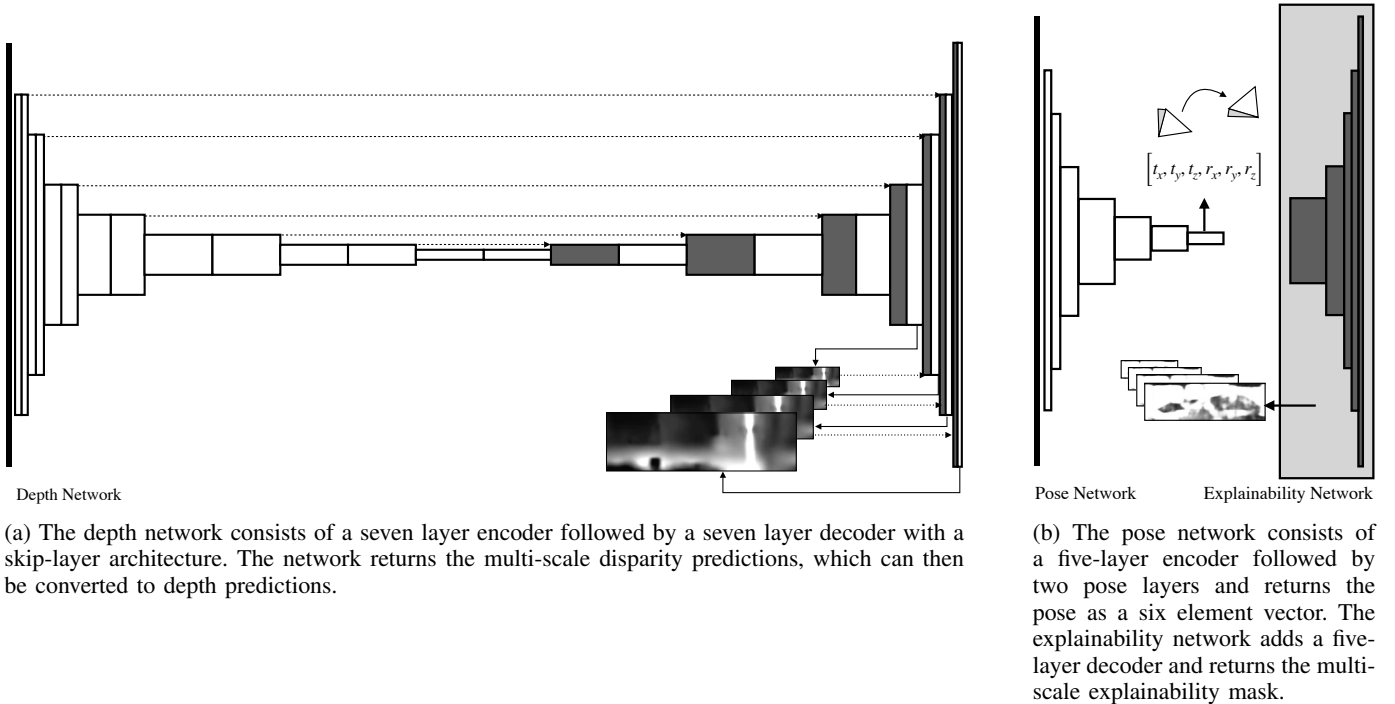


Fig. 3: The SfMLearner model consists of two jointly-trained CNN stacks. The left diagram shows the depth CNN, and the right diagram shows the pose/explainability CNN.

drical panoramas do not capture the full 3D space. However, they have a major benefit: they can be mapped exactly to a plane, removing the issue of polar distortion. Despite this benefit, little research has been done using deep networks with the cylindrical projection model [9], [20]. Furthermore, while some spherical CNN networks have made simplifications, including cropping of the polar regions [4] and distortion-aware filters [4], to the best of our knowledge, no previous work has applied a cylindrical CNN to the structure-from-motion problem. Our work introduces the first CNN model designed to predict depth and pose from cylindrical panoramic input.

III. METHODS

In this work, we present an unsupervised convolutional model that jointly estimates the depth map from a single cylindrical panoramic image and ego-motion from image sequences.

A. Model Architecture

Our architecture is based on that of Zhou et. al [30], an unsupervised model designed to predict depth and ego-motion in monocular pinhole images. The architecture, illustrated in Figure 3, is a convolutional network consisting of two jointly-trained stacks: (a) a depth network to estimate the depth map, (b) a pose network/explainability mask to estimate the change in the pose in image sequences and handle unexplainable input. The depth network follows the DispNet [17] skip-layer architecture, with seven contracting layers and seven expanding layers, outputting a multi-scale depth prediction.

The pose network (PoseExpNet) consists of five contracting convolutional layers and three pose layers, outputting the predicted translation and rotation between the source and target views. The explainability network consists of a final five upconvolution layers and returns a multi-scale explainability mask, which masks “unexplainable” motion.

The learner uses *view synthesis*—the prediction of a target frame given source frames—as an internal supervisor. At each step, the joint DispNet and PoseExpNet stacks predict the depth of a target frame and the pose difference between the target and source frames. The depth and pose are then used for synthesizing a target view: as the predicted view improves the depth and pose predictions also improve [30]. This process is illustrated in Figure 4.

For this model, we use a three-part objective function. The main component is the *photometric loss* ($\mathcal{L}_{\text{pixel}}$), which minimizes the difference between synthesized views and the target view, which, in turn, improves the depth and pose predictions. This is regularized by the *smooth loss* ($\mathcal{L}_{\text{smooth}}$), which minimizes the second derivatives with respect to the depth and the *explainability loss* (\mathcal{L}_{exp}), which makes the model more resilient to anomalous input (e.g. moving objects). If λ_s and λ_e represent the smooth and explainability weights, the total loss can be written as follows:

$$\mathcal{L} = \sum_{\text{scales}} \left(\sum_{\text{sources}} \mathcal{L}_{\text{pixel}} + \lambda_s \mathcal{L}_{\text{smooth}} + \sum_{\text{sources}} \lambda_e \mathcal{L}_{\text{exp}} \right) \quad (1)$$

If \mathcal{I} is an RGB image, \mathcal{D} is the depth prediction, and e

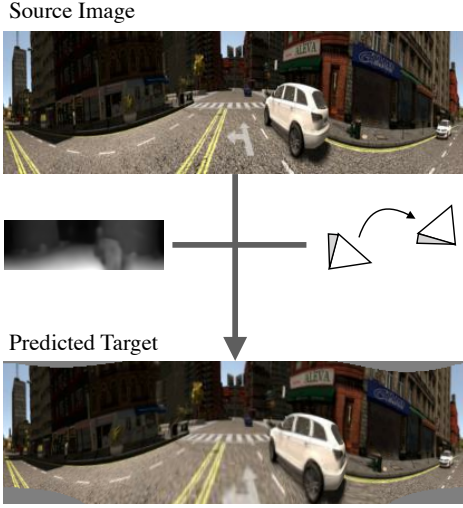


Fig. 4: We use panoramic view synthesis as a supervisor: the source panorama, depth, and pose transformation are used to synthesize a target view, and the loss is computed as the difference between the actual and synthesized views. As the synthesized view improves, the depth and pose predictions improve.

is the explainability mask, the three loss components can be written as follows:

$$\mathcal{L}_{\text{pixel}} = \frac{\sum e |\mathcal{I}_{\text{proj}} - \mathcal{I}_{\text{target}}|}{\|\mathcal{I}_{\text{target}}\|} \quad (2)$$

$$\mathcal{L}_{\text{smooth}} = \left| \frac{\delta^2 \mathcal{D}}{\delta x^2} \right| + \left| \frac{\delta^2 \mathcal{D}}{\delta x \delta y} \right| + \left| \frac{\delta^2 \mathcal{D}}{\delta y \delta x} \right| + \left| \frac{\delta^2 \mathcal{D}}{\delta y^2} \right| \quad (3)$$

$$\mathcal{L}_{\text{exp}} = \sum \text{softmax}(\mathcal{E}) \quad (4)$$

Two major modifications were required to allow for cylindrical input: (a) the intrinsics and view synthesis functions were modified to account for cylindrical projection, and (b) the convolutional layers, resampling functions, and loss were modified to preserve horizontal wrapping.

1) *Camera Projection and Cylindrical Panoramas*: Our view synthesis function works by (a) projecting a source image onto the 3D sensor coordinate system, (b) inverse warping the points from the source pose to target pose, and (c) projecting the warped points back onto a 2D image plane. To adapt this process to work with cylindrical input, we modified the mapping functions between the pixel, camera, and world coordinate frames.

Most structure-from-motion systems expect *pinhole projection* images as input. Pinhole projection images project a 3D scene from the world coordinate system onto a flat image plane; this process can be described by the focal length f , principle point c , the image plan height H , and the image plane width W , as shown in Figure 5.

In contrast, *cylindrical projection* projects the 3D world onto a curved cylindrical surface, as seen in Figure 6. The goal of this process is to take a 3D point in the world

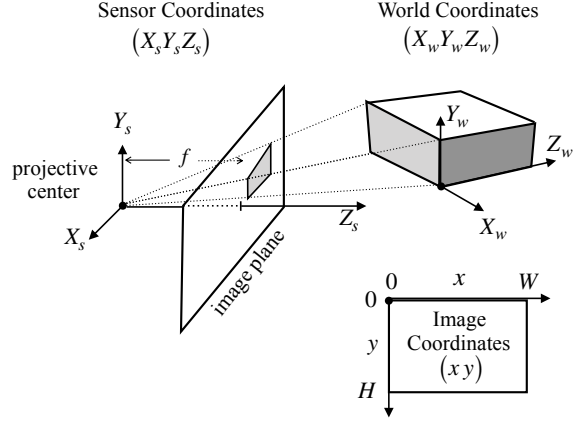


Fig. 5: Pinhole projection model. The 3D world (on the world coordinate system) is projected on a flat image plane; the image plane is a focal length f away from the projective center along the Z_s axis (on the sensor coordinate system). The result is an $W \times H$ rectangular image.

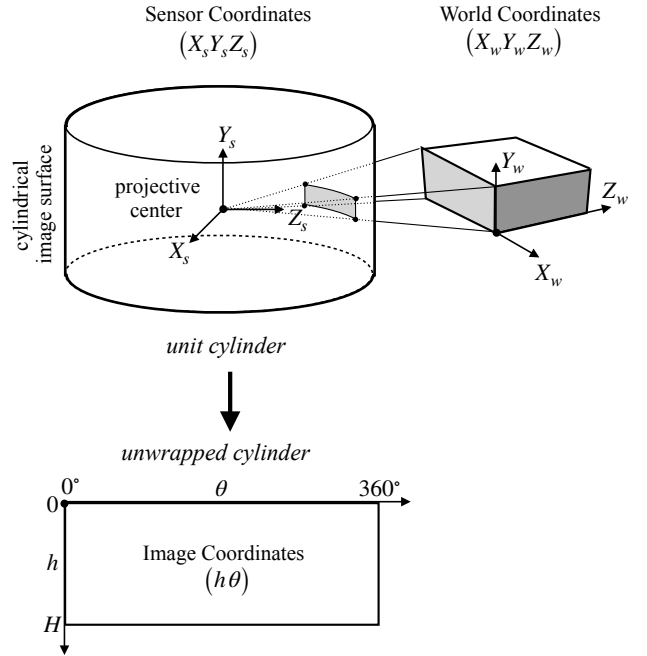


Fig. 6: Cylindrical projection model. In contrast with pinhole projection, this projects an image onto a curved cylindrical surface. The final result is a rectangular image with height H and a width representing the full 360° .

coordinate system and project it onto a rectangular cylindrical panorama. This requires projecting the 3D point onto the cylindrical image surface and converting the image surface into a Cartesian coordinate system.

The transformation between the sensor and pixel coordinate systems can be described by the following equations: let $P = (x_s, y_s, z_s)$ represent a point in the 3D sensor coordinate system $X_s Y_s Z_s$. We can find point $Q = (r, \theta, h)$, the point where P is projected onto a unit cylinder around the origin,

with the following formula:

$$\begin{bmatrix} r \\ \theta \\ h \end{bmatrix} = \begin{bmatrix} 1 \\ \arctan\left(\frac{x_s}{z_s}\right) \\ \frac{y_s}{\sqrt{x_s^2 + z_s^2}} \end{bmatrix} \quad (5)$$

This can be represented by the 2D point $q = (\theta, h)$.

To "unroll" this cylinder into a rectangular image with the Cartesian system xy , we must use some camera intrinsics: scaling factor f ; output width W ; output height H ; principle point (c_x, c_y) . The following equations will convert $q = (\theta, h)$ into $p = (x, y)$:

$$\begin{bmatrix} x \\ y \end{bmatrix} = \begin{bmatrix} \frac{\theta}{2\pi}W + c_x \\ fH + c_y \end{bmatrix} \quad (6)$$

The final panoramic image has a fixed height H and a width of W (representing the full 360° view), as seen in Figure 6.

The reverse projection ($P = (x_s, y_s, z_s)$ given $q = (\theta, h)$ and some scaling factor d) can be described as follows:

$$\begin{bmatrix} x_s \\ y_s \\ z_s \end{bmatrix} = \begin{bmatrix} d \sin \theta \\ dh \\ d \cos \theta \end{bmatrix} \quad (7)$$

The cylindrical intrinsics \mathcal{K} can be represented by the following matrix:

$$\mathcal{K} = \begin{bmatrix} f_\theta & 0 & c_\theta \\ 0 & f_h & c_h \\ 0 & 0 & 1 \end{bmatrix} \quad (8)$$

Let θ represent the field of view, x represent the horizontal pixel position, h represent the height coverage, and y represent the vertical pixel position. Then we can find the intrinsics values with the following formulas:

$$f_\theta = \frac{\theta_0 x_1 - x_0 \theta_1}{\theta_0 - \theta_1} \quad (9)$$

$$c_\theta = \frac{x_0 - x_1}{\theta_0 - \theta_1} \quad (10)$$

$$f_h = \frac{h_0 y_1 - y_0 h_1}{h_0 - h_1} \quad (11)$$

$$c_h = \frac{y_0 - y_1}{h_0 - h_1} \quad (12)$$

2) *Horizontal Wrapping*: In order to extend the model for cylindrical panoramic images, we modified the convolutional layers, smooth loss function, and 2D projection to account for horizontal wrapping.

In a cylindrical image, the left and right side of the input image are adjacent. For a convolutional layer to work with cylindrical input, it must preserve this horizontal wrapping property. This can be done by padding the right side of the tensor with columns from the left and vice-versa, as illustrated in Figure 7.

We implemented a cylindrical 2D convolution function which wraps the normal 2D convolution function in Tensorflow and adds horizontal wrap padding. The cylindrical

convolution replaces all normal convolutions in the network architecture. We also added wrap padding to the smooth gradient loss, ensuring the depth is smooth between the two sides of the unwrapped depth image, and the bilinear sampler, ensuring that the synthesized views take the full 360° into account.

IV. EXPERIMENTS

Several experiments were performed to determine the performance of cylindrical panoramic networks. First, to determine the effect of increasing the field of view on prediction accuracy, we trained and evaluated CylindricalSfMLearner on increasing slices of the panoramas: 100°, 180°, 270°, 360° without horizontal wrapping, and 360° with horizontal wrapping. Next, to demonstrate the model's effectiveness on real-world footage, we trained and tested the network on a new self-collected dataset.

CylindricalSfMLearner was implemented in the open-source machine learning library Tensorflow [1]. Our code will be made publicly available on GitHub.

A. Monocular Depth Estimation

While there are many standard datasets such as KITTI [10] and CityScapes [5] that provide standard field-of-view video with registered ground truth depth, we were unable to find a similar dataset containing panoramic video and associated ground truth with suitable characteristics. For this reason, we performed a quantitative evaluation of our work on synthetic data.

1) *SYNTHIA-Seqs*: SYNTHIA-Seqs [19] is a synthetic dataset of driving data designed to mimic the properties of popular front-view datasets like KITTI [10] and CityScapes [5]. For this experiment, we used sequences 02 and 05 (NYC-like city driving) in the spring-, summer-, and fall-like conditions captured from the left and right stereo cameras.

To prepare the data for training, we first stitched the four perspective views into a single 360° cylindrical panorama using basic geometric techniques. Next, we identified static frames using the global pose ground truth; these frames were excluded from the final formatted dataset using the same

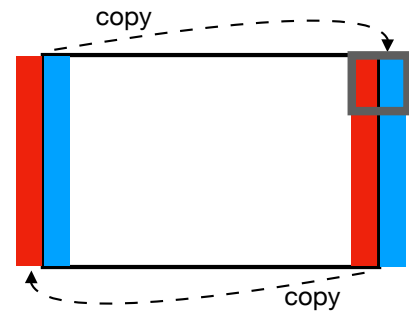


Fig. 7: An example of a horizontally wrapping convolutional layer. The wrapping is achieved by copying the left-most columns to the right side and vice-versa.

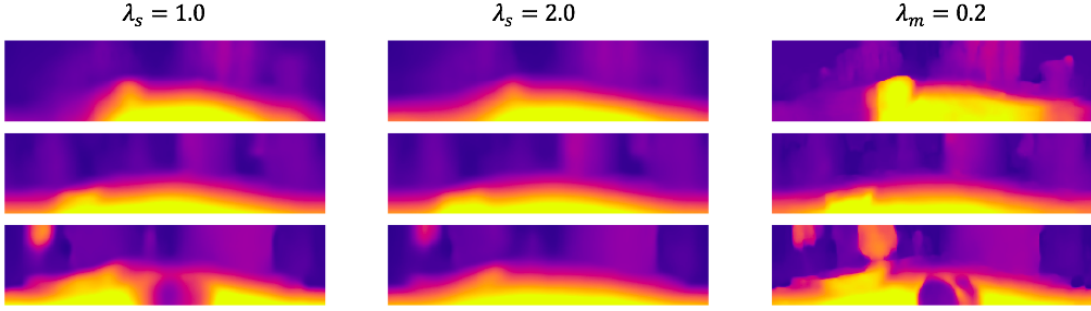


Fig. 8: A comparison of different loss functions. The first and second columns represent second-order depth gradient loss at different weights: $\lambda_s = 1.0$ and $\lambda_s = 2.0$. The rightmost column shows an image-aware first-order gradient loss with a weight $\lambda_m = 0.2$.

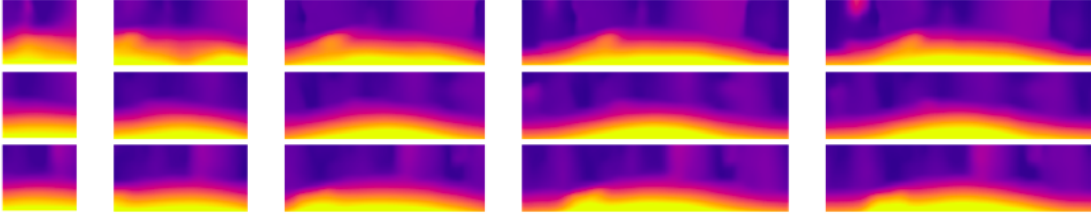


Fig. 9: A visual comparison of Synthia predictions with different field of views (from left: 100°, 180°, 270°, 360° unwrapped, and 360° wrapped).

technique as SfMLearner [30]. Panoramas were then resized to 512×128 and concatenated to form three-frame sequences. After processing, this dataset contained 4,398 panoramic views. This was split into train, test, and validation subsets comprised of approximately 80%, 10%, and 10% of the data, respectively.

We experimented with various settings of the smoothing term and also alternative smoothing terms such as the image-aware first-order gradient loss from Mahjourian et al.[16]. A comparison is shown in Figure 8. We found that while increasing the smoothness reduces the detail in the depth prediction, it tended to increase the depth accuracy. For the remaining experiments on Synthia we chose a smoothness term of $\lambda_s = 2.0$ and $\lambda_e = 0$ and trained all models for 60,000 steps.

2) *Increasing the Field of View:* Model performance was evaluated in 100°, 180°, 270°, 360° unwrapped, and 360° wrapped panoramas. These new FoV datasets were created by cropping the 360° panoramas, centered around the direction of motion, and updating the corresponding camera intrinsics. These panoramas were then stitched into sequences using the technique described above. The images were resized as follows: 100° FoVs were resized to 144×128 , 180° FoVs were resized to 256×128 , and 270° FoVs were resized to 384×128 .

We used a set of disparity and accuracy metrics common in SfM research that each capture a different aspect of the prediction error; for more details, please refer to [7].

As can be seen in Table I, large field of views consistently perform better than small field of views on accuracy measures (right columns). They have mixed performance in disparity

measures: the 100° FoV outperforms larger FoVs on squared relative error, a metric that strongly penalizes large outliers; however, the wrapped 360° FoV performs better on RMSE log, a metric that emphasizes shallow depth predictions. Additionally, 360° input consistently performed better with horizontal wrapping than without.

We were surprised by the performance of the 180° and 270° FoVs; they often beat both the 100° and 360° models in disparity metrics. We believe that this may be due to the road taking up a smaller proportion of these views; it would be interesting to investigate this trend further in future work.

3) *Qualitative Evaluation with Real Data:* While the SYNTHIA-Seqs dataset allowed us to explore the effect of cylindrical projection and increasing field of views, its major limitation is that it is a synthetic dataset. In order to determine if cylindrical projection is successful with real-world input, we trained and evaluated a model on our own panoramic dataset.

This model was trained with the same configuration as above with the exception of the smooth loss term. This model was trained using image-aware smooth loss ($\lambda_m = 0.2$) [16] as opposed to the second-order gradient loss. This change helps to improve the definition of predicted object shapes such as trees and cars.

a) *Headcam Dataset:* We assembled a panoramic video dataset which we call Headcam. It was collected by affixing a consumer-grade panoramic camera, the 2016 Samsung Gear 360, to a bicycle helmet and biking around neighborhoods in Northern Virginia. This dataset includes about two hours of footage, and it was collected over a one-week period. We will release this dataset publicly for future use by other researchers.

Field of View	Disparity (lower is better)				Accuracy (higher is better)		
	Abs Rel	Sq Rel	RMSE	RMSE log	$\delta < 1.25$	$\delta < 1.25^2$	$\delta < 1.25^3$
100°	0.2529	1.9990	7.3771	0.3869	0.6358	0.8097	0.8957
180°	0.2708	1.9495	6.1822	0.3778	0.6470	0.8233	0.9036
270°	0.3031	2.2353	5.9202	0.3969	0.6480	0.8194	0.8979
360°	0.3016	2.5437	6.2202	0.3958	0.6689	0.8280	0.9011
360° (wrapped)	0.2994	2.5149	6.0375	0.3870	0.6757	0.8358	0.9065

TABLE I: Depth accuracy results when training and testing our network architecture on different fields of view input. The model trained on the complete 360 deg field-of-view with horizontal wrapping has the most accurate depth predictions according to the delta threshold metrics (right columns).

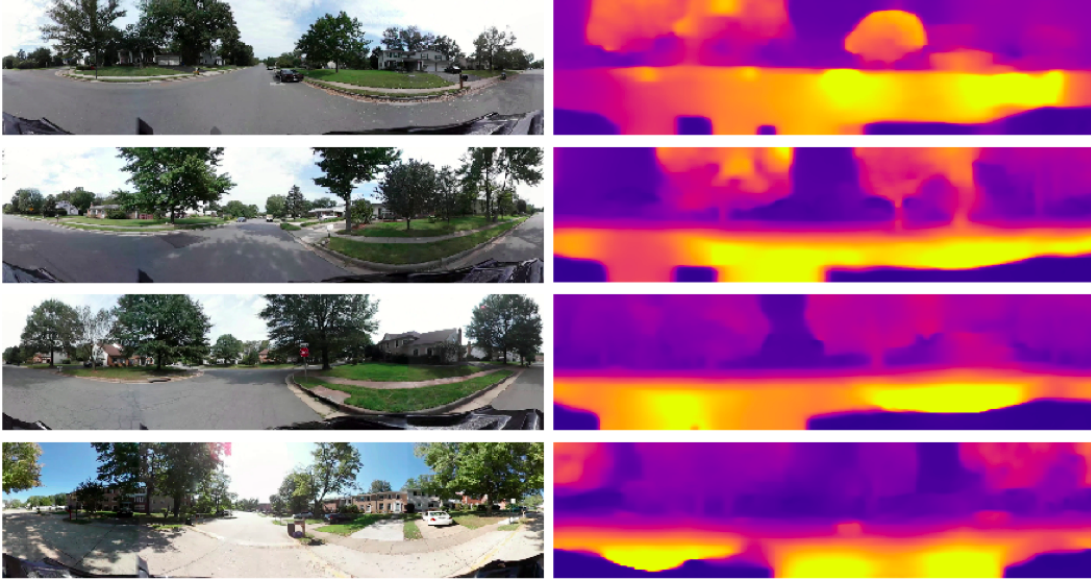


Fig. 10: Depth predictions for the self-collected headcam dataset. Our cylindrical CNN model achieves highly detailed depth predictions on panoramic input. The missing depth predictions at the bottom are due to the helmet being visible in the frame.

This footage was first stitched into equirectangular panoramic video using the Samsung Gear 360 software. It was then broken into frames at 5fps, warped into a cylindrical projection model, resized to 512×128 , and formatted into three-frame sequences. The final formatted dataset contains 27,275 usable frames. Training was conducted on 90% of the data, and qualitative testing was done on the remaining 10%.

Predictions on the test set can be seen in Figure 10. Qualitatively, the model generates visually reasonable predictions with well-defined object boundaries. However, the model makes several common errors. Most notably, due to its constant presence frame-to-frame, the model predicts that the helmet at the bottom of the image has a large depth. Future work might explore ways to mitigate this through masking or other techniques. We also noticed occasional holes in the depth prediction in the road, similar to the predictions on Synthia when using a low smoothing term.

V. CONCLUSION

We introduce the first unsupervised model for learning depth and ego-motion directly from panoramic video input. In contrast to previous work, we use the cylindrical panoramic projection which allows for direct application of existing

convolutional neural network models to panoramic input with little modification. Our evaluation on synthetic and real data shows that learning from cylindrical panoramic input is as effective as pinhole projection input in producing accurate and detailed depth predictions.

We also contribute a novel dataset of real panoramic video suitable for unsupervised learning of depth and ego-motion. The dataset was captured on city streets from a helmet-mounted camera while riding a bicycle and thus contains a variety of motions, moving objects, and other challenging conditions, making it a difficult and interesting dataset for future research on learning panoramic structure-from-motion.

While the cylindrical projection makes the application of convolutional neural networks to panoramic input simple, there are some limitations to this representation. First, the top and bottom of the complete spherical field-of-view are not included in the cylindrical representation; however, in most applications, these regions are not important. Second, our model does not achieve full rotation invariance like, for example, the Spherical CNN model of Cohen et al. [3]. Our cylindrical CNN model is invariant to rotation about the vertical axis (yaw) but not rotation about the other two axes (pitch and roll). However, pitch and roll rotations of the camera are relatively

rare in street-level driving tasks as evaluated in this paper. Full rotation invariance could be more important for other applications such as processing head-mounted camera video captured during extreme sports or video from a flying drone. In future work, we would like to delve into this more deeply and investigate when cylindrical panoramas are a reasonable representation (e.g. SfM for level motion) and when spherical panoramas might be better (e.g. UAV flight).

Future work could also include a comparison of our cylindrical model against the various spherical CNN models that have been proposed, and experimenting with other state-of-the-art depth prediction architectures [28], [27] adapted for cylindrical panoramic input. One weakness of our model was depth prediction accuracy in low-texture areas, and further work could be done to experiment with the loss function and model structure to improve performance in these low texture areas.

Future work also includes developing a panoramic video dataset with 360° footage and registered ground truth depth data similar to existing perspective-image datasets [10], [5] to benefit future research on panoramic depth estimation.

Finally, we note that depth estimation from panoramic video offers many future applications to explore, such as low-power robotic navigation and production of stereoscopic virtual reality video from monocular input.

ACKNOWLEDGMENTS

We would like to thank the University of Colorado: Colorado Springs for their support and computing resources. This material is based upon work supported by the National Science Foundation under Grant Nos. 1659788 and 1464420.

REFERENCES

- [1] M. Abadi, A. Agarwal, P. Barham, E. Brevdo, Z. Chen, C. Citro, G. S. Corrado, A. Davis, J. Dean, M. Devin, S. Ghemawat, I. Goodfellow, A. Harp, G. Irving, M. Isard, Y. Jia, R. Jozefowicz, L. Kaiser, M. Kudlur, J. Levenberg, D. Mané, R. Monga, S. Moore, D. Murray, C. Olah, M. Schuster, J. Shlens, B. Steiner, I. Sutskever, K. Talwar, P. Tucker, V. Vanhoucke, V. Vasudevan, F. Viégas, O. Vinyals, P. Warden, M. Wattemberg, M. Wicke, Y. Yu, and X. Zheng. TensorFlow: Large-scale machine learning on heterogeneous systems, 2015. Software available from tensorflow.org.
- [2] J. R. Bergen, P. Anandan, K. J. Hanna, and R. Hingorani. Hierarchical model-based motion estimation. In *European Conf. Computer Vision*, pages 237–252. Springer, 1992.
- [3] T. S. Cohen, M. Geiger, J. Koehler, and M. Welling. Spherical CNNs. In *Int. Conf. Learning Representations*, Vancouver, Canada, 2018.
- [4] B. Coors, A. P. Condurache, and A. Geiger. SphereNet: Learning Spherical Representations for Detection and Classification in Omnidirectional Images. In *European Conf. Computer Vision*, page 16, 2018.
- [5] M. Cordts, M. Omran, S. Ramos, T. Rehfeld, M. Enzweiler, R. Benenson, U. Franke, S. Roth, and B. Schiele. The cityscapes dataset for semantic urban scene understanding. In *Proc. IEEE Conf. Computer Vision and Pattern Recognition*, pages 3213–3223, 2016.
- [6] G. P. de La Garanderie, A. A. Abarghouei, and T. P. Breckon. Eliminating the Blind Spot: Adapting 3d Object Detection and Monocular Depth Estimation to 360° Panoramic Imagery. In *European Conf. Computer Vision*, Aug. 2018.
- [7] D. Eigen, C. Puhrsch, and R. Fergus. Depth map prediction from a single image using a multi-scale deep network. In *Advances in Neural Information Processing Systems*, pages 2366–2374, 2014.
- [8] C. Esteves, C. Allen-Blanchette, A. Makadia, and K. Daniilidis. Learning SO(3) Equivariant Representations with Spherical CNNs. In *European Conf. Computer Vision*, pages 52–68, 2018.
- [9] C. Esteves, C. Allen-Blanchette, X. Zhou, and K. Daniilidis. Polar Transformer Networks. In *Int. Conf. Learning Representations*, 2018.
- [10] A. Geiger, P. Lenz, and R. Urtasun. Are we ready for autonomous driving? The KITTI vision benchmark suite. In *Proc. IEEE Conf. Computer Vision and Pattern Recognition*, pages 3354–3361. IEEE, 2012.
- [11] C. Godard, O. Mac Aodha, and G. J. Brostow. Unsupervised monocular depth estimation with left-right consistency. In *Proc. IEEE Conf. Computer Vision and Pattern Recognition*, volume 2, page 7, 2017.
- [12] J. Huang, Z. Chen, D. Ceylan, and H. Jin. 6-DOF VR videos with a single 360-camera. In *IEEE Transactions on Visualization and Computer Graphics*, pages 37–44. IEEE, 2017.
- [13] R. Khasanova and P. Frossard. Graph-based classification of omnidirectional images. In *IEEE International Conference on Computer Vision Workshops (ICCVW)*, pages 860–869, 2017.
- [14] V. R. Kumar, S. Milz, C. Witt, M. Simon, K. Amende, J. Petzold, S. Yogamani, and T. Pech. Near-field Depth Estimation using Monocular Fisheye Camera: A Semi-supervised learning approach using Sparse LIDAR Data. In *Deep Vision: Beyond Supervised Learning*, page 3, June 2018. Extended Abstract.
- [15] F. Liu, C. Shen, G. Lin, and I. Reid. Learning depth from single monocular images using deep convolutional neural fields. *IEEE Transactions on Pattern Analysis and Machine Intelligence*, 38(10):2024–2039, 2016.
- [16] R. Mahjourian, M. Wicke, and A. Angelova. Unsupervised learning of depth and ego-motion from monocular video using 3d geometric constraints. In *Proc. IEEE Conf. Computer Vision and Pattern Recognition*, 2018.
- [17] N. Mayer, E. Ilg, P. Hausser, P. Fischer, D. Cremers, A. Dosovitskiy, and T. Brox. A large dataset to train convolutional networks for disparity, optical flow, and scene flow estimation. In *Proc. IEEE Conf. Computer Vision and Pattern Recognition*, pages 4040–4048, 2016.
- [18] R. Mur-Artal, J. M. M. Montiel, and J. D. Tardos. ORB-SLAM: a versatile and accurate monocular SLAM system. *IEEE Transactions on Robotics*, 31(5):1147–1163, 2015.
- [19] G. Ros, L. Sellart, J. Materzynska, D. Vazquez, and A. M. Lopez. The SYNTHIA dataset: A large collection of synthetic images for semantic segmentation of urban scenes. In *Proc. IEEE Conf. Computer Vision and Pattern Recognition*, pages 3234–3243. IEEE, June 2016.
- [20] H. Salehinejad, S. Naqvi, E. Colak, J. Barlett, and S. Valaei. Cylindrical Transform: 3d Semantic Segmentation of Kidneys With Limited Annotated Images. In *IEEE Global Conference on Signal and Information Processing*, Sept. 2018.
- [21] A. Saxena, M. Sun, and A. Y. Ng. Make3d: Learning 3d scene structure from a single still image. *IEEE Transactions on Pattern Analysis and Machine Intelligence*, 31(5):824–840, 2009.
- [22] Y.-C. Su and K. Grauman. Learning spherical convolution for fast features from 360 imagery. In *Advances in Neural Information Processing Systems*, pages 529–539, 2017.
- [23] K. Tateno, N. Navab, and F. Tombari. Distortion-Aware Convolutional Filters for Dense Prediction in Panoramic Images. In *European Conf. Computer Vision*, page 16, 2018.
- [24] S. Vijayanarasimhan, S. Ricco, C. Schmid, R. Sukthankar, and K. Fragkiadaki. Sfm-net: Learning of structure and motion from video. *arXiv preprint arXiv:1704.07804*, 2017.
- [25] C. Wang, J. M. Buenaposada, R. Zhu, and S. Lucey. Learning depth from monocular videos using direct methods. In *Proc. IEEE Conf. Computer Vision and Pattern Recognition*, pages 2022–2030, 2018.
- [26] M. Weiler, F. A. Hamprecht, and M. Storath. Learning Steerable Filters for Rotation Equivariant CNNs. In *Proc. IEEE Conf. Computer Vision and Pattern Recognition*, page 10, 2018.
- [27] D. Xu, W. Wang, H. Tang, H. Liu, N. Sebe, and E. Ricci. Structured attention guided convolutional neural fields for monocular depth estimation. In *Proc. IEEE Conf. Computer Vision and Pattern Recognition*, pages 3917–3925, 2018.
- [28] Z. Yin and J. Shi. GeoNet: Unsupervised learning of dense depth, optical flow and camera pose. In *Proc. IEEE Conf. Computer Vision and Pattern Recognition*, volume 2, 2018.
- [29] Q. Zhao, C. Zhu, F. Dai, Y. Ma, G. Jin, and Y. Zhang. Distortion-aware CNNs for Spherical Images. In *Proc. Int. Joint Conf. Artificial Intelligence*, pages 1198–1204, Stockholm, Sweden, July 2018. International Joint Conferences on Artificial Intelligence Organization.
- [30] T. Zhou, M. Brown, N. Snavely, and D. G. Lowe. Unsupervised learning of depth and ego-motion from video. In *Proc. IEEE Conf. Computer Vision and Pattern Recognition*, volume 2, page 7, 2017.